Mesh r-adaptation for unilateral contact problems

Pierre Béal, Jonas Koko, Rachid Touzani

Mesh r–adaptation for unilateral contact problems *

Pierre Béal † Jonas Koko ‡ Rachid Touzani §

Abstract

We present a mesh adaptation method by node movement for two-dimensional linear elasticity problems with unilateral contact. The adaptation is based on a hierarchical estimator on finite element edges and the node displacement techniques use an analogy of the mesh topology with a spring network. We show, through numerical examples, the efficiency of the present adaptation method.

Key Words : Unilateral contact, Linear elasticity, Mesh Adaptivity, Node movement.

1 Introduction

In contact mechanics the determination of the contact region is often a challenging issue. This one generally depends on the algorithm of contact detection and its accuracy closely depends on the mesh size. For these reasons, it seems natural to consider very fine meshes in the neighborhood of this unknown region by making use of mesh adaptation techniques.

The aim of this paper is to present an algorithm of topology preserving mesh adaptation. This one is based on node movement rather than mesh classical refinement/coarsening techniques. The choice of this so-called r–adaptation strategy is motivated at least by two reasons : node movement techniques preserve matrix structure and are then well suited for large size computations, *e.g.*, three-dimensional and/or nonlinear cases. Moreover, these ones are well adapted for differentiation with respect to node positions in order to calculate sensitivities like for shape optimization for instance.

r–adaptation techniques are not new but are not so popular in the numerical analysis literature. The reason for this is their lack of flexibility and their ability to generate unesthetic meshes with a risk of degeneracy. We show in the present work that much accuracy can be recovered by slightly concentrating the mesh

*This work was supported by the MFP Michelin.

†NUMTECH – 27, rue Jean Claret, Parc Technologique de La Pardieu, 63 063 Clermont-Ferrand Cedex 1, France – E-mail : beal@numtech.fr

‡Laboratoire d'Informatique, de Modélisation et d'Optimisation, des Systèmes – CNRS / FRE 2239, Université Blaise Pascal (Clermont-Ferrand II), 63 177 Aubière Cedex, France – E-mail : koko@isima.fr

§Corresponding author: Laboratoire de Mathématiques Appliquées – CNRS / UMR 6620, Université Blaise Pascal (Clermont-Ferrand II), 63 177 Aubière Cedex, France – E-mail : touzani@math.univ-bclermont.fr – Fax : +33 4 73 40 70 64.

in the regions where "something happens", for instance in the contact region and especially in the vicinity of its boundary where contact pressure fails to be smooth. It turns out that one can mainly distinguish in the literature two types of r–adaptation formulations.
The first one consists in formulating the mesh adaptation problem as an energy minimization one, the optimization parameters being the solution of the boundary value problem as well as the position of mesh nodes. This approach is clearly possible only if the boundary value problem is equivalent to a minimization one which is the case for frictionless contact elasticity problems. Such a method was studied in Haslinger et al. [1992] where mathematical results of existence of an optimal mesh are proved. In Tourigny – Hülsemann [1998], the authors give an iteration procedure to obtain the optimal mesh. The method is essentially based on a Gauss-Seidel like method. Our tests show that although the method is attractive since well adapted for the problem formulation, the iteration algorithm seems to diverge in situations and even in the cases where it converges, edge swapping of the triangles is required. This constraint obviously alters the mesh topology. Let us note that, in addition, that all optimization approaches contain a difficulty related to the fact that the nondegeneracy of the triangulation must be imposed as a constraint in the problem and that this constraint must be satisfied at each iteration of the optimization process. This issue requires than the use of interior penalty method which significantly complicates the setting of the mesh adaptation problem.
We have adopted, in the present work, an adaptation technique based on hierarchical estimators. In other words, we use higher order interpolation to evaluate local errors. It is noteworthy that edge based errors are well suited for contact problems for their ability to generate anisotropic meshes. These ones have been introduced mainly in Habashi et al. [1996], D'azevedo [1991] and D'azevedo and Simpson [1991]. We have formulated these techniques the case of a mesh r–adaptation procedure. It turns out that, with some restrictions that will be outlined in the paper, the adaptation allows using a moderately coarse mesh with an acceptable accuracy.
The paper is organized as follows : in the following section, we present a model linear plane strain elasticity problem with a Signorini's contact condition. We define a standard finite element approximation of the problem and an iteration procedure to solve the discretized contact problem. Section 3 is devoted to the presentation of the mesh adaptation procedure. In particular, an important issue is the recovery of the hessian of the approximate solution. The mesh movement algorithm is also described. Section 4 presents some numerical tests to confirm the validity and efficiency of the method. Finally, Section 5 draws some conclusions about the described method and some possible future developments.

2 Position of the Problem

In this section, we recall the setting of a unilateral contact Signorini's problem for linear elasticity.
We consider a deformable body occupying in its reference configuration a domain Ω of $\mathbb{R}^2$ with boundary Γ divided into three disjoined subsets Γ_D, Γ_N and Γ_C. We consider furthermore a rigid obstacle described by the curve $x_2 = \phi(x_1)$.

We assume that the domain, in its reference configuration, is located "above" the obstacle, *i.e.*

$$x_2 \geq \phi(x_1) \qquad \text{for all } \boldsymbol{x} = (x_1, x_2) \in \Omega.$$

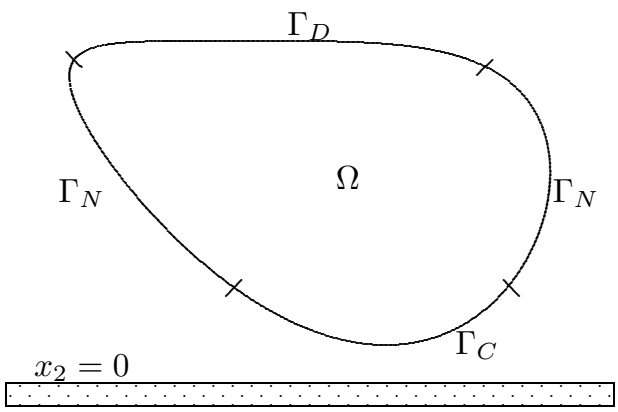

Figure 1: A unilateral contact problem ($\phi(x_1) = 0$)

Let d denote the *contact distance* function defined by

$$d(\boldsymbol{u})(\boldsymbol{x}) := \phi(x_1) - x_2 - u_2(\boldsymbol{x}),$$

where $\boldsymbol{u}(\boldsymbol{x}) = (u_1(\boldsymbol{x}), u_2(\boldsymbol{x}))$ is the displacement of the point $\boldsymbol{x}$. The set of admissible displacements is defined by

$$\mathcal{V} := \{\boldsymbol{v} \in H^1(\Omega; \mathbb{R}^2);\ \boldsymbol{v} = 0 \text{ on } \Gamma_D,\ d(\boldsymbol{v}) \leq 0 \text{ on } \Gamma_C\},$$

where $H^1(\Omega; \mathbb{R}^2)$ is the space of vector valued functions $\boldsymbol{v}$ such that

$$\int_\Omega \left(|\boldsymbol{v}|^2 + \left|\frac{\partial \boldsymbol{v}}{\partial x_1}\right|^2 + \left|\frac{\partial \boldsymbol{v}}{\partial x_2}\right|^2 \right) d\boldsymbol{x} < +\infty.$$

Here above, we have imposed to the deformed domain to be above the obstacle. Moreover, we have imposed a Dirichlet boundary condition on Γ_D and a traction free boundary condition on Γ_N. We assume moreover that the boundary Γ_D does not interact with the obstacle in the deformed configuration. The energy functional is given by

$$W : \boldsymbol{v} \in \mathcal{V} \mapsto W(\boldsymbol{v}) = \frac{1}{2} a(\boldsymbol{v}, \boldsymbol{v}) - \int_\Omega \boldsymbol{f} \cdot \boldsymbol{v}\, d\boldsymbol{x} - \int_{\Gamma_N} \boldsymbol{g} \cdot \boldsymbol{v}\, ds \in \mathbb{R},$$

where a is the bilinear symmetric form defined by the linear elasticity problem. Namely,

$$a(\boldsymbol{u}, \boldsymbol{v}) = \sum_{i,j,k,l=1}^{2} \int_\Omega c_{ijkl} \varepsilon_{ij}(\boldsymbol{u}) \varepsilon_{ij}(\boldsymbol{v})\, d\boldsymbol{x}, \tag{2.1}$$

and $\boldsymbol{f}$ (*resp.* $\boldsymbol{g}$) is a smooth function that stands for the applied body (*resp.* boundary) force. In (2.1), (c_{ijkl}) is the tensor of elastic coefficients and

$$\varepsilon_{ij}(\boldsymbol{u}) = \frac{1}{2}\left(\frac{\partial u_i}{\partial x_j} + \frac{\partial u_j}{\partial x_i}\right) \qquad 1 \leq i, j \leq 2$$

is the symmetric tensor of infinitesimal deformations. We choose here the case of an isotropic and homogeneous material, *i.e.* (c_{ijkl}) is given by

$$c_{ijkl} = \mu(\delta_{ik}\delta_{jl} + \delta_{il}\delta_{jk}) + \lambda\delta_{ij}\delta_{kl} \qquad 1 \leq i, j, k, l \leq 2,$$

the real numbers $\lambda \geq 0$ and $\mu > 0$ denoting Lamé coefficients of the material, and δ_{ij} is the Kronecker delta. These coefficients are related in plane deformations to the Young modulus E and Poisson coefficient ν by relationships :

$$\lambda = \frac{\nu E}{(1+\nu)(1-2\nu)}, \ \mu = \frac{E}{2(1+\nu)}.$$

The equilibrium problem consists in seeking a minimum of the functional W :

$$\text{Find } \boldsymbol{u} \in \mathcal{V} \quad \text{such that} \quad W(\boldsymbol{u}) \leq W(\boldsymbol{v}) \qquad \text{for all } \boldsymbol{v} \in \mathcal{V}. \tag{2.2}$$

It is well known (cf. Kikuchi – Oden [1988]) that the solution of Problem (2.2) satisfies the variational inequality :

$$\begin{cases} \boldsymbol{u} \in \mathcal{V}, \\ a(\boldsymbol{u}, \boldsymbol{v} - \boldsymbol{u}) \geq \displaystyle\int_\Omega \boldsymbol{f} \cdot (\boldsymbol{v} - \boldsymbol{u})\, d\boldsymbol{x} \\ \qquad\qquad + \displaystyle\int_{\Gamma_N} \boldsymbol{g} \cdot (\boldsymbol{v} - \boldsymbol{u})\, ds \quad \text{for all } \boldsymbol{v} \in \mathcal{V}. \end{cases}$$

2.1 The discrete problem

Let us consider now a finite element approximation of Problem (2.2). We assume that the domain Ω is polygonal and we consider a triangulation $\mathcal{K}^h$ of Ω into triangles of diameters $\leq h$. We define the space

$$\mathcal{X}^h = \{\boldsymbol{v} \in \mathcal{C}^0(\overline{\Omega}; \mathbb{R}^2);\ \boldsymbol{v}_{|K} \in (P_1)^2 \text{ for all } K \in \mathcal{K}^h,\ \boldsymbol{v} = 0 \text{ on } \Gamma_D\},$$

where P_1 is the space of affine polynomials. Let $(\boldsymbol{a}^i)_{1 \leq i \leq I}$ denote the set of nodes on Γ_C. We define furthermore, for $\boldsymbol{v} \in \mathcal{X}^h$ the contact distance at nodes $\boldsymbol{a}^i$ of Γ_C by $d_i(\boldsymbol{u}) := d(\boldsymbol{u})(\boldsymbol{a}^i)$, $1 \leq i \leq I$. We define the set :

$$\mathcal{V}^h := \{\boldsymbol{v} \in \mathcal{X}^h;\ d_i(\boldsymbol{v}) \leq 0,\ 1 \leq i \leq I\}.$$

Notice that here, the set $\mathcal{V}^h$ is not included in $\mathcal{V}$. This feature is at the origin of some numerical difficulties in contact problems.
For each function $\boldsymbol{v} \in \mathcal{X}^h$, we define a function $d^h(\boldsymbol{v})$ on Γ_C, continuous, piecewise linear and that coincides with $d_i(\boldsymbol{v})$ at node $\boldsymbol{a}^i$, for all $i \in \{1, \ldots, I\}$.
The discrete problem is defined by :

$$\text{Find } \boldsymbol{u}^h \in \mathcal{V}^h \quad \text{such that} \quad W(\boldsymbol{u}^h) \leq W(\boldsymbol{v}) \quad \text{for all } \boldsymbol{v} \in \mathcal{V}^h. \tag{2.3}$$

2.2 A penalty solution method

In order to solve the constrained optimization problem (2.3), we use a standard external penalty method. For this, we define for $\varepsilon > 0$ the penalized energy functional

$$W_\varepsilon(\boldsymbol{v}) := W(\boldsymbol{v}) + \frac{1}{2\varepsilon} \int_{\Gamma_C} (d^h(\boldsymbol{v})^+)^2\, ds.$$

The penalized problem is defined by :

$$\text{Find } \boldsymbol{u}^h \in \mathcal{X}^h \quad \text{such that} \quad W_\varepsilon(\boldsymbol{u}^h) \leq W_\varepsilon(\boldsymbol{v}) \qquad \text{for all } \boldsymbol{v} \in \mathcal{X}^h. \tag{2.4}$$

It is well known and easy to prove that the unique solution of Problem (2.4) converges, in the energy norm, to the solution to Problem (2.3) when $\varepsilon \to 0$. Here, the principal interest of the penalized problem (2.4) is that the nonpenetration constraint is removed. It can be also shown that the solution to Problem (2.4) solves the variational problem :

$$\begin{cases} \boldsymbol{u}^h \in \mathcal{X}^h, \\ a(\boldsymbol{u}^h, \boldsymbol{v}) + \dfrac{1}{\varepsilon} \displaystyle\int_{\Gamma_C} d^h(\boldsymbol{u}^h)^+ v_2 \, ds \quad = \displaystyle\int_\Omega \boldsymbol{f} \cdot \boldsymbol{v} \, d\boldsymbol{x} + \displaystyle\int_{\Gamma_N} \boldsymbol{g} \cdot \boldsymbol{v} \, ds \\ \qquad\qquad\qquad\qquad\qquad\qquad\qquad\qquad \text{for all } \boldsymbol{v} \in \mathcal{X}^h. \end{cases}$$

The obtained problem is thus a nonlinear one due to the nonlinearity of the boundary integral in the variational formulation (2.5). It remains then to build an iterative scheme to solve the nonlinearity.

2.3 An iteration procedure

In order to solve the nonlinear problem (2.5), we consider the following simple iteration scheme :

$$\begin{cases} \text{Given } (\boldsymbol{u}^h)^n \in \mathcal{X}^h, \\ \text{Find } (\boldsymbol{u}^h)^{n+1} \in \mathcal{X}^h \text{ such that} \\ a((\boldsymbol{u}^h)^{n+1}, \boldsymbol{v}) + \dfrac{1}{\varepsilon} \displaystyle\int_{\Gamma_C} \alpha^n d^h((\boldsymbol{u}^h)^{n+1}) v_2 \, ds = \displaystyle\int_\Omega \boldsymbol{f} \cdot \boldsymbol{v} \, d\boldsymbol{x} + \displaystyle\int_{\Gamma_N} \boldsymbol{g} \cdot \boldsymbol{v} \, ds \\ \qquad\qquad\qquad\qquad\qquad\qquad\qquad\qquad \text{for all } \boldsymbol{v} \in \mathcal{X}^h, \end{cases}$$

for $n = 0, 1, 2, \ldots$, where

$$\alpha^n = \begin{cases} 1 & \text{if } d^h((\boldsymbol{u}^h)^n) > 0, \\ 0 & \text{otherwise.} \end{cases}$$

Hence, the iteration procedure consists, for each iteration step, in detecting contact for each node by using displacements at the previous iteration.
Numerical experiments have shown good properties of this iteration process : in all cases convergence is achieved in some iterations.

Remark 2.1. Although the penalty term involves integrals of polynomials of degree 2, we use to evaluate it the trapezoidal rule in order to avoid well known numerical locking.

3 Mesh r-Adaptation

Let us define our r–adaptation method. This one uses, like most of mesh adaptation algorithms, an *a posteriori* error estimator. The estimator here is said to be hierarchical in the sense that it is based on a P_2–approximation of the

solution. The presented method was developed by Peraire et al. [1992], Habashi et al. [1996], D'azevedo and Simpson [1991], and Fortin [1998]. This one is often used for an h–adaptation method, *i.e.* adaptation by mesh refinement of coarsening. We use it here for an r–adaptation.
Let us present the method as briefly as possible, the details can be found in papers by Peraire et al. [1992], Habashi et al. [1996], D'azevedo and Simpson [1991], Fortin [1998]. Consider a triangle K and a polynomial $\widetilde{u}^h$ of degree 2 on K. In practice, $\widetilde{u}^h$ will stand for the restriction to K of a piecewise P_2 approximation of the solution of the problem. We consider furthermore the P_1–interpolate of $\widetilde{u}^h$, denoted by u^h. let $e^h = \widetilde{u}^h - u^h$. It can be shown (D'azevedo and Simpson [1991]) that the error function e is proportional to the hessian $\boldsymbol{H}$ of $\widetilde{u}^h$. Using this property, we adopt the following adaptation criterion : We seek a mesh that achieves an equidistribution of the error e^h on the edges of the triangulation. Therefore, if E is an edge of the triangulation and if $\boldsymbol{\tau}_E$ is the unit tangent to E, the second derivative along the $\boldsymbol{\tau}_E$–direction is given by

$$\frac{\partial^2 \boldsymbol{u}}{\partial \boldsymbol{\tau}_E^2} = \boldsymbol{\tau}_E^T \boldsymbol{H} \boldsymbol{\tau}_E.$$

Let $\boldsymbol{x}_k$ and $\boldsymbol{x}_\ell$ denote the two vertices of the edge E. If the (constant) matrix $\boldsymbol{H}$ is semi–positive definite, we define the error estimator on E by

$$e_{k\ell} = (\boldsymbol{a}_{k\ell}^T \boldsymbol{H} \boldsymbol{a}_{k\ell})^{\frac{1}{2}}.$$

Note that, in the case where $\boldsymbol{H}$ is positive definite, this error defines a new metric on the edge E. In this case, error equidistribution on the edges is equivalent to prescribe the all edges have the same length in the metric associated to $\boldsymbol{H}$.

3.1 Practical computation of the estimator

The calculation of the error $e_{k\ell}$ can be achieved in the following way : We have if $\boldsymbol{g}$ is the gradient of $\widetilde{u}^h$ and if we note that this one is an affine vector on the edge E :

$$\boldsymbol{H}\boldsymbol{a} = \begin{pmatrix} \boldsymbol{a}_{k\ell}^T \dfrac{\partial \boldsymbol{g}}{\partial x_1} \\ \\ \boldsymbol{a}_{k\ell}^T \dfrac{\partial \boldsymbol{g}}{\partial x_2} \end{pmatrix} = \frac{\partial \boldsymbol{g}}{\partial \boldsymbol{a}_{k\ell}} = \boldsymbol{g}_k - \boldsymbol{g}_{k\ell},$$

where $\boldsymbol{g}_k = \boldsymbol{g}(\boldsymbol{x}_k)$.
When the matrix $\boldsymbol{H}$ is not semi-positive definite, we consider (as in Fortin [1998]) the spectral decomposition of $\boldsymbol{H}$:

$$\boldsymbol{H} = \boldsymbol{R}^T \boldsymbol{\Lambda}\, \boldsymbol{R},$$

where $\boldsymbol{\Lambda}$ is the diagonal matrix of eigenvalues of $\boldsymbol{H}$. Let us denote by $|\boldsymbol{\Lambda}|$ the matrix obtained from $\boldsymbol{\Lambda}$ by replacing the eigenvalues by their absolute values and by $|\boldsymbol{H}|$ the matrix

$$|\boldsymbol{H}| = \boldsymbol{R}^T |\boldsymbol{\Lambda}|\, \boldsymbol{R}.$$

Using the inequality

$$|\boldsymbol{b}^T \boldsymbol{H}\, \boldsymbol{b}| \leq \boldsymbol{b}^T |\boldsymbol{H}|\, \boldsymbol{b} \qquad \text{for all } \boldsymbol{b} \in \mathbb{R}^2,$$

we replace the hessian matrix $\boldsymbol{H}$ by $|\boldsymbol{H}|$. We now want to calculate the error

$$e_{k\ell} = (\boldsymbol{a}_{k\ell}^T |\boldsymbol{H}| \boldsymbol{a}_{k\ell})^{\frac{1}{2}}$$

using $\widetilde{u}^h$. We have, if $\widehat{\boldsymbol{a}}_{ij} = \boldsymbol{R}\boldsymbol{a}_{ij}$ and $\widehat{\boldsymbol{g}} = \boldsymbol{R}\boldsymbol{g}$:

$$\begin{aligned} \boldsymbol{a}_{k\ell}^T |\boldsymbol{H}| \boldsymbol{a}_{k\ell} &= \boldsymbol{a}_{k\ell}^T \boldsymbol{R}^T |\boldsymbol{\Lambda}| \boldsymbol{a}_{k\ell} \\ &= \boldsymbol{a}_{k\ell}^T \boldsymbol{R}^T (|\widehat{\boldsymbol{g}}_k| - |\widehat{\boldsymbol{g}}_\ell|) \\ &= \boldsymbol{a}_{k\ell}^T \boldsymbol{R}^T (|\boldsymbol{R}\boldsymbol{g}_k| - |\boldsymbol{R}\boldsymbol{g}_\ell|). \end{aligned} \tag{3.1}$$

It remains now to calculate the hessian. The difficulty resides in the fact that, since the approximate solution u^h is only continuous, its second partial derivatives are Dirac distributions on element edges. To approximate these distributions we proceed as follows : A continuous approximation of the hessian matrix entries is obtained by the following projection :

$$H_{ij}(\boldsymbol{x}_k) \approx \frac{\displaystyle\int_{\Omega_k} \frac{\partial^2 u^h}{\partial x_i \partial x_j} \phi_k \, d\boldsymbol{x}}{\displaystyle\int_{\Omega_k} \phi_k \, d\boldsymbol{x}}, \tag{3.2}$$

where ϕ_k is the basis function associated to node $\boldsymbol{x}_k$ and Ω_k is the union of triangles that share this node. Let us point out that the above integrals are actually duality brackets since, as previously mentioned, the second order derivatives of the approximate solution are only distributions. Effective calculation of the above expression is then obtained by use of the Green's formula :

$$H_{ij}(\boldsymbol{x}_k) \approx \frac{\displaystyle\int_{\Gamma_k} \frac{\partial u^h}{\partial x_i} \phi_k n_j \, ds - \int_{\Omega_k} \frac{\partial u^h}{\partial x_i} \frac{\partial \phi_k}{\partial x_j} \, d\boldsymbol{x}}{\displaystyle\int_{\Omega_k} \phi_k \, d\boldsymbol{x}},$$

where Γ_k is the union of boundaries of triangles of Ω_k, and $\boldsymbol{n} = (n_i)$ is the outward unit normal to the edges Γ_k.

3.2 Node displacement Procedure

Let us now define an algorithm to move the nodes according to the computed edge errors. We have adopted for this a classical technique that considers the finite element mesh as a network of elastic springs with stiffness coefficients that depend on the error estimator on each edge (cf. Habashi et al. [1996]). In this technique, node positions are interpreted as the solution of an energy minimization problem. The Hooke's law for this spring network is given by

$$\sum_{\ell=1}^{n} (\boldsymbol{x}_\ell - \boldsymbol{x}) \kappa_\ell(\boldsymbol{x}) = 0. \tag{3.3}$$

where $\kappa_\ell(\boldsymbol{x})$ is the constant of spring with ends $\boldsymbol{x}$ and $\boldsymbol{x}_\ell$. The dependency of this one on the estimator is empirically chosen as

$$\kappa_\ell(\boldsymbol{x}) = \frac{e_\ell(\boldsymbol{x})}{\|\boldsymbol{x}_\ell - \boldsymbol{x}\|},$$

where $e_\ell(\boldsymbol{x})$ is the metric of the edge of vertices $\boldsymbol{x}$ and $\boldsymbol{x}_\ell$; in particular, $e_\ell(\boldsymbol{x}_k) = \boldsymbol{a}_{k\ell} = \boldsymbol{x}_k - \boldsymbol{x}_\ell$. In order to solve the nonlinear equation (3.3), we use a relaxation procedure, *i.e.*, we update node positions by the iteration procedure :

$$\boldsymbol{x}^{p+1} = \boldsymbol{x}^p + \omega \, \frac{\displaystyle\sum_{\ell=1}^{n} (\boldsymbol{x}_\ell - \boldsymbol{x}^p)\kappa_\ell(\boldsymbol{x}^p)}{\displaystyle\sum_{\ell=1}^{n} \kappa_\ell(\boldsymbol{x}^p)}, \qquad p = 0, 1, \ldots$$

where ω is the relaxation parameter. In practice, we do not iterate until complete convergence, *i.e.*, we iterate until an acceptable discrepancy (10^{-3}, say) is obtained.

Remark 3.1. The case of boundary nodes is treated separately. Here we project the computed new position of each boundary node on the actual boundary. Let us note that another difficulty is related to the fact that boundary nodes define the actual boundary of the domain. Any displacement of these nodes modifies hence this boundary.

3.3 Remarks

1. Numerical experimentation of this method shows that this one is *a priori* only valid for structured meshes, *i.e.*, meshes with a constant node connectivity. This difficulty can be explained by the fact that error equidistribution on the edges does not coincide with energy minimization of the spring network in the unstructured case. Numerical tests have shown poor behavior in the unstructured case.

2. In practice, convergence of the iteration process depends on the relaxation parameter ω. Obviously, a small value of ω ensures convergence but with a large number of iterations. Moreover, a limitation on the node displacements must be included in the procedure in order to prevent elements from degeneracy. This constraint is simply implemented by prescribing relative upper and lower bounds on edge lengths.

3.4 Numerical tests

In order to validate the previously described adaptation method, we first present a simple test on an explicitly given function and then give two elasticity contact problems.

3.4.1 A validation test

Consider the domain $\Omega = (0,1) \times (0,1)$ of $\mathbb{R}^2$. We construct a uniform mesh by dividing each edge of Ω into 10×10 sub-intervals. The adaptation of this mesh for the function

$$f(\boldsymbol{x}) = e^{-10\, x_1 + x_2}.$$

is given in Fig. 2. The number of iterations was 51 for a value of $\omega = 0.8$.
We have also tested the behavior of the node movement procedure when using quadrilateral Q_1 elements, the obtained mesh is plotted in Fig. (3). We note

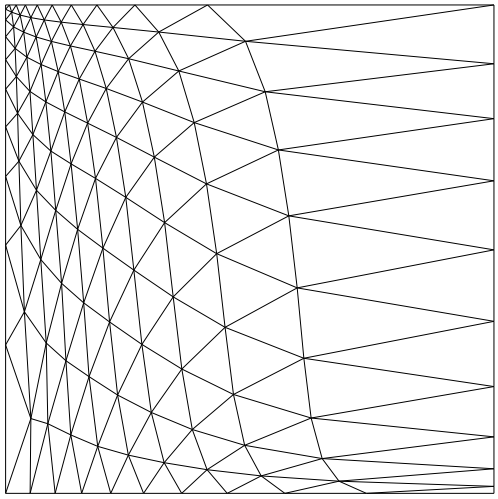

Figure 2: Adapted mesh (case P_1)

here that the orthogonality of the mesh is preserved after adaptation. This is due to the separation of variables in the tested function f. For this example, the number of iterations was 49 for a value of $\omega = 0.8$.

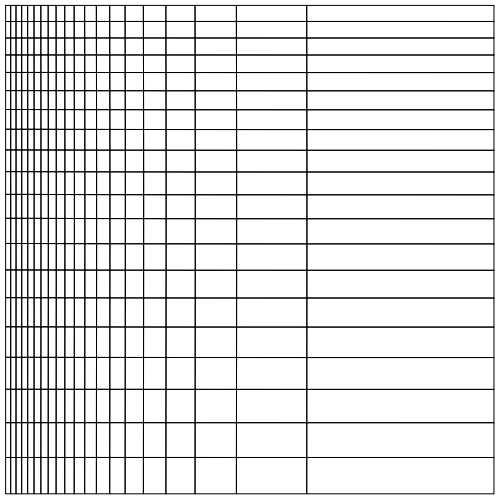

Figure 3: Adapted mesh (case Q_1)

3.4.2 A cantilever beam

We consider a cantilever beam defined by the domain $\Omega = (0, 4) \times (0.05, 1)$ clamped at its end $x_1 = 0$ and submitted at its top side $x_2 = 1$ to a normal traction p. The beam is furthermore in potential contact with a rigid horizontal obstacle defined by the line $x_2 = 0$. We choose the data :

$$p = -100, \; E = 2\,000, \; \nu = 0.3.$$

Figure 4 presents a uniform coarse mesh of the beam.

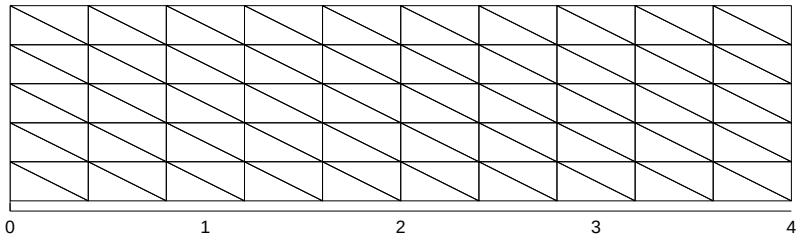

Figure 4: Cantilever beam : A uniform mesh

The adaptation algorithm produces the mesh plotted in Figure 5.

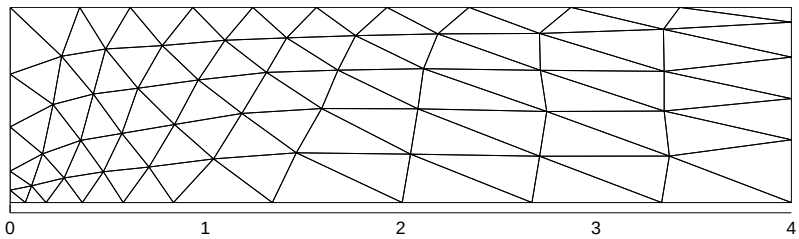

Figure 5: Cantilever beam : Adapted mesh

We have compared the contact pressure at the bottom $x_2 = 0$ with the one obtained with the coarse mesh (Fig. 6) and with a fine mesh (320 triangles). Figure 5 shows that, on the one hand, the mesh is displaced in the neighborhood of the boundary of the contact region. On the other hand, the contact pressure is, as expected, more accurate for the adapted mesh than for the initial one.

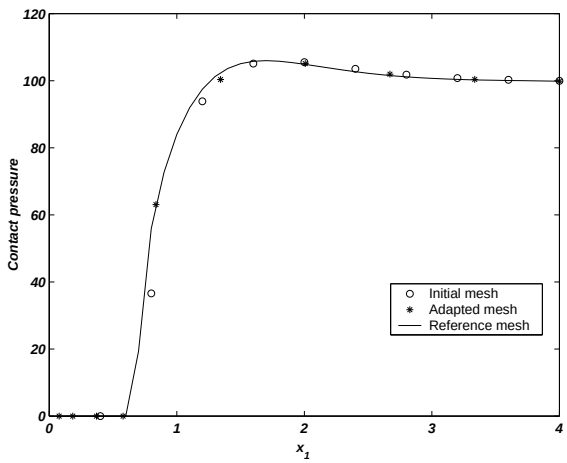

Figure 6: Cantilever beam : Comparison of contact pressures

3.4.3 The Hertz test

A classical test in the numerical simulation of contact mechanics is the Hertz contact problem. Let us recall that this one consists in a disk in contact with a horizontal obstacle. The disk is submitted along its radius to a uniform pressure f. The details can be found in Kikuchi – Oden [1988] for instance. It is shown that if the radius is "large enough" then the half width of the contact region is given by

$$b = 2\sqrt{\frac{fR(1-\nu^2)}{\pi E}}$$

and the contact pressure is given by

$$p(\boldsymbol{x}) = \frac{2f}{\pi b^2}\sqrt{b^2 - x_1^2}, \qquad \boldsymbol{x} \in \Gamma_C.$$

Computations are carried out using a half disk with radius $R = 8$. Figure 7 illustrates the initial mesh of the domain in its reference configuration while Figures 8 and 9 illustrate the adapted mesh in the reference and deformed configurations respectively. We can note that the adaptation process has refined the mesh in the contact region and particularly at the boundary of this region where the contact pressure admits a discontinuity of the gradient. This was clearly the main goal of the present study.

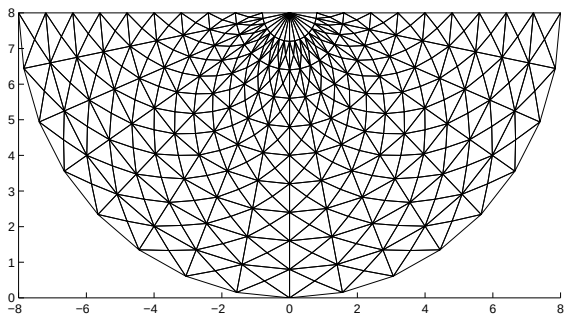

Figure 7: Hertz Test : Initial mesh

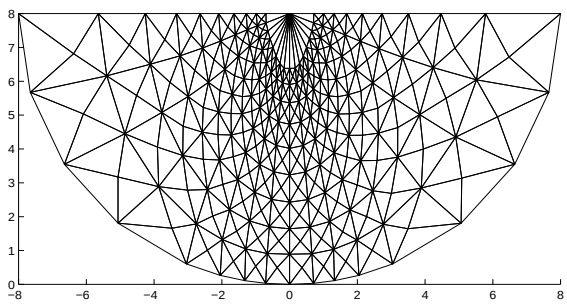

Figure 8: Hertz Test : Adapted mesh

The efficiency of the method appears more clearly when one considers the calculated contact pressures and the determination of the contact region (Fig. 10).

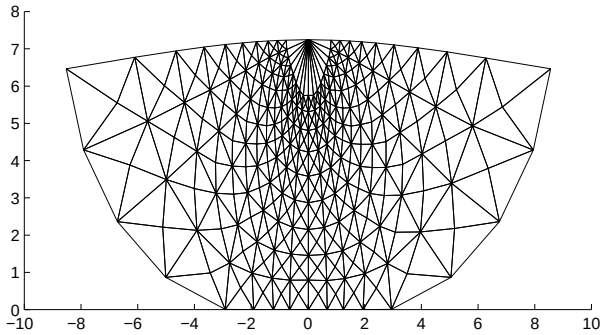

Figure 9: Hertz Test : Adapted mesh (Deformed configuration)

This one is numerically identified as the set of nodes where the boundary traction is not vanishing.

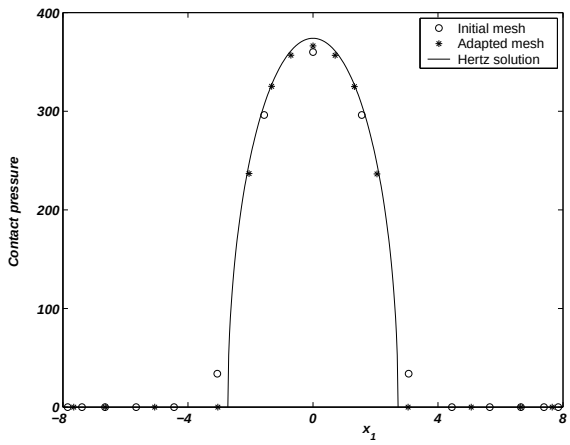

Figure 10: Hertz Test : Comparison of contact pressures

3.4.4 A disk test

We present here a test inspired by the contact of a car wheel on a rigid obstacle standing for a road. The tire is idealized by an elastic disk Ω of radius 0.5. The obstacle is materialized by the line $x_2 = 0$. Elastic properties are given by

$$E = 10^7, \ \nu = 0.45.$$

Finally, the "wheel" is assumed to be submitted to a vertical displacement at its center equal to $u_2 = -0.05$. This singular condition ideally models the connection between the wheel and other parts of the vehicle.
Figures 11 and 12 show respectively the initial and adapted mesh of the reference configuration.
Clearly, the mesh concentrates about the center where a singularity occurs due to the prescribed vertical displacement. In addition, as expected, a refinement

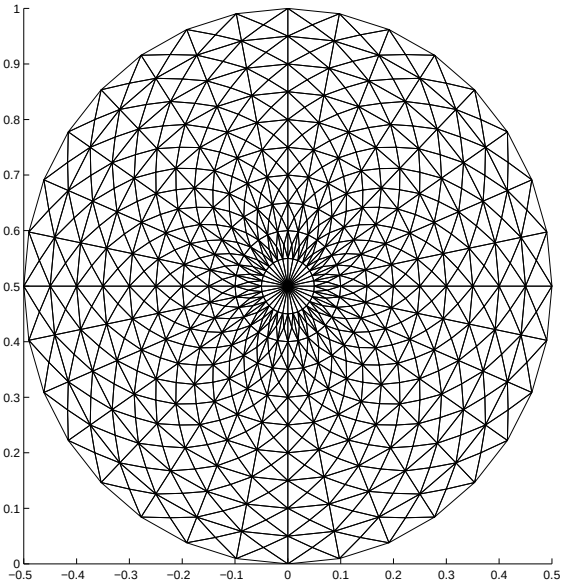

Figure 11: Disk Test : Initial Mesh

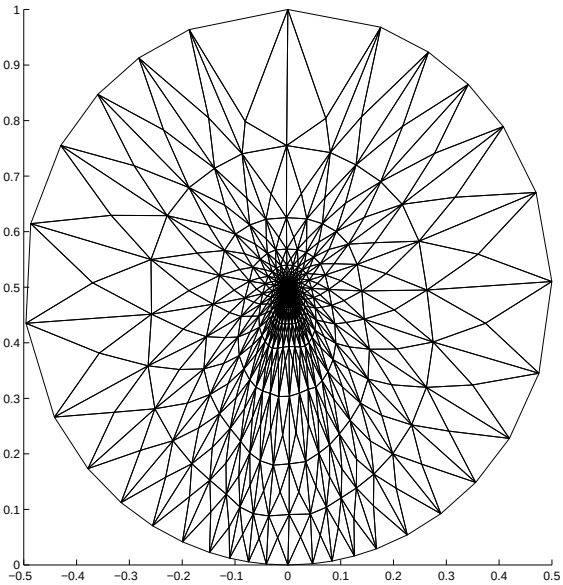

Figure 12: Disk Test : Adapted Mesh

occurs in the contact region as well as around the singularity that occurs at the disk center. We can also note that the mesh symmetry around the axis $x_1 = 0$ is almost perfectly preserved. Further calculation with a nonsymmetric mesh has given bad results. Figure 13 shows a comparison of contact pressures at contact nodes. We have compared the solution obtained for the initial and adapted meshes (made of 1184 elements) and a reference solution obtained with a very

fine mesh (the disk is partitioned into 200 sectors and 50 layers, yielding 39400 elements). This figure shows that, except for the maximal pressure point, the obtained adapted pressure is very close to the reference one and, as for the Hertz test, the result is more spectacular for contact detection. It is also noticeable that this result is obtained for a very coarse mesh.

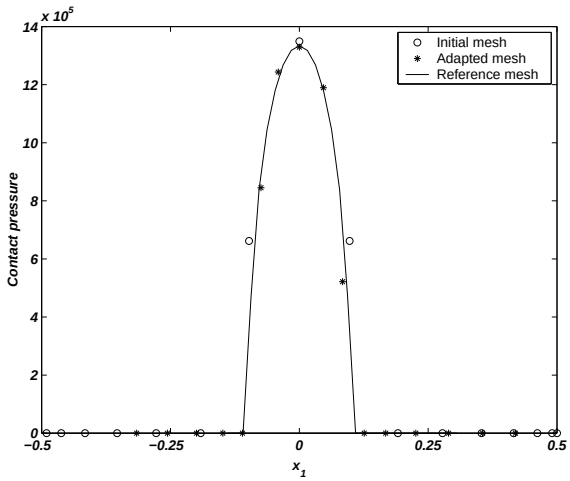

Figure 13: Disk Test : Comparison of contact pressures

4 Conclusion

We have developed an r–adaptation mesh method that enabled solving with sufficient accuracy a unilateral contact elasticity problem. This method has as an advantage its simplicity and its modularity since this one is completely independent of the solver (the method actually works for all elliptic linear and nonlinear problems). Its main drawback is its limitation to structured meshes (triangular and quadrilateral). We can conjecture this is mainly due to the analogy of the finite element mesh with a spring network. A promising issue is the replacement of this analogy with the solution of a boundary value problem.

Acknowledgments. The authors are deeply indebted to C. Rahier et A. Rezgui from the MFP Michelin for fruitful discussions.

References

D'azevedo, E. F. (1991): *Optimal triangular mesh generation by coordinate transformation* — SIAM J. Sci. Stat. Comput., Vol.12, No.4, pp.755-786.

D'azevedo, E. F. – Simpson, R. B. (1991): *On optimal triangular meshes for minimizing the gradient error* — Nümerische Mathematik, Vol.59, No.4, pp.321-348.

Fortin, M. (1998): *Anisotropic mesh adaptation through hierarchical error estimators* — SIAM J. Numer. Anal., Vol.26, No.4, pp.788-811.

Habashi, W. G., Fortin, M., Yahia, D. A.-A., Boivin, S., Bourgault, Y., Dompierre, J., Robichaud, M. P., Tam, A., and Vallet, M.-G. (1996): *Anisotropic mesh optimization. Towards a solver-independent and mesh-independent CFD* — Lecture Series in Computational Fluid Dynamics, Von Karman Institute for Fluid Dynamics.

Haslinger, J., Neitaanmäki, P., and Salmenjoki, K. (1992): *On FE-grid relocation in solving unilateral boundary value problems by fem* — Applications of Mathematics, Vol.37, No.2, pp.105-122.

Kikuchi, N. and Oden, J. (1988): *Contact Problems in Elasticity : A Study of Variational Inequalities and Finite Element Methods* — SIAM, Philadelphia, PA.

Peraire, J., Perió, J., and Morgan, K. (1992): *Adaptive remeshing for three-dimensional compressible flow computation* — J. Comp. Phys., Vol.103, pp.269-285.

Tourigny, Y. and Hülsemann, F. (1998): *A new moving mesh algorithm for the finite element solution of variational problems* — SIAM J. Numer. Anal., Vol.35, No.4, pp.1416-1438.